Journal of Catalysis **198,** 151–163 (2001)
doi:10.1006/jcat.2000.3132, available online at http://www.idealibrary.com on IDEAL®

The Effect of Support Interaction on the Sulfidability of Al_2O_3- and TiO_2-Supported CoW and NiW Hydrodesulfurization Catalysts

M. J. Vissenberg,* Y. van der Meer,† E. J. M. Hensen,* V. H. J. de Beer,* A. M. van der Kraan,† R. A. van Santen,* and J. A. R. van Veen*,[1]

*Schuit Institute of Catalysis, Eindhoven University of Technology, P.O. Box 513, 5600 MB Eindhoven, The Netherlands; and †Interfacultair Reactor Instituut, Delft University of Technology, Mekelweg 15, 2629 JB Delft, The Netherlands

Received November 24, 1999; revised September 4, 2000; accepted November 17, 2000; published online February 13, 2001

The effect of the degree of W sulfidation on dispersion, morphology, thiophene hydrodesulfurization (HDS) activity, and promotional behavior for supported Ni(Co)W sulfide catalysts was studied by varying the calcination temperature, sulfidation temperature, sulfidation pressure, and support. The catalysts were characterized by thiophene HDS, X-ray photoelectron spectroscopy; transmission electron microscopy, extended X-ray absorption fine-structure, and Mössbauer emission measurements. Assuming that sulfidation to a WS_2 phase proceeds via a WO_xS_y phase it can be concluded that the ratio between these two phases depends on the sulfidation conditions and W–support interaction. For the highest thiophene HDS activity, sulfidation conditions that result in nearly maximum sulfidation of the WO_xS_y phase are necessary. However, one should be aware that complete sulfidation results in the formation of WS_2, which is more susceptible to sintering. For Al_2O_3-supported NiW catalysts preferable sulfidation conditions are a low temperature and a high H_2S/H_2 sulfidation pressure. In contrast, for TiO_2-supported NiW the calcination and sulfidation temperatures have to be low and sulfidation at atmospheric H_2S/H_2 pressure is already sufficient, because W is more easily sulfided due to its weak interaction with TiO_2. The degree of sulfidation also affects the promotional behavior. The optimal Ni/W ratio is higher than the optimal Ni/Mo ratio, while in contrast to CoMo catalysts, for CoW no optimal ratio could be found. In addition, the activity of CoW appeared about the same as the sum of the W and Co activities, regardless of the Co content. In the case of NiW and CoW, Ni and Co are sulfided first. As soon as WS_2 appears, the NiS particles already formed partially redisperse to form NiWS, while the CoS particles tend to form a separate Co_9S_8 phase instead of CoWS. © 2001 Academic Press

Key Words: **NiW sulfide; CoW sulfide; alumina; titania; support interaction; sulfidability; hydrodesulfurization.**

INTRODUCTION

Al_2O_3-supported Ni(Co)Mo and NiW sulfide catalysts are widely used in the oil industry for hydrotreating processes. Interestingly, the sulfidation behavior and catalytic properties of the promoted W- and Mo-based catalysts are clearly different.

First, NiW/Al_2O_3 was reported to be much more difficult to sulfide than $NiMo/Al_2O_3$ (1–3). In addition, the optimum sulfidation degree was found (1, 2, 4) to depend on the type of reaction for which the catalyst was used. According to Breysse *et al.* (1, 2) maximum hydrogenation activity was obtained after incomplete sulfidation while for hydrodesulfurization (HDS) or hydrodenitrogenation (HDN) reactions complete sulfidation provided optimum activity. Reinhoudt *et al.* (4) showed that complete sulfidation of W resulted in the highest thiophene HDS activity (tested in gas phase), while the highest dibenzothiophene HDS activity (tested in trickle flow) was found for incompletely sulfided W. An extensive sulfidation study of NiW/Al_2O_3 (4–7) led to the conclusion that application of higher calcination temperatures retards the formation of WS_2 slabs and that this calcination temperature effect can be compensated for by raising the sulfidation temperature sufficiently.

Second, as reflected in the composition and availability of commercial catalysts, W and Mo behave differently on addition of Ni or Co. Ni appears to be an effective promoter for both W/Al_2O_3 and Mo/Al_2O_3, albeit that the Ni/W ratio required for optimal promotion is higher than the corresponding Ni/Mo ratio. The promotion effect of Co is strikingly lower for W/Al_2O_3 than for Mo/Al_2O_3.

The study reported in this paper specifically deals with W-based catalysts and the results are discussed in the light of the two aspects mentioned above. The relation between sulfidation degree and activity was studied by variation of calcination temperature, sulfidation temperature, and pressure, W–support interaction (Al_2O_3 (relatively strong) versus TiO_2 (relatively weak) (8)). The catalysts were characterized by X-ray photoelectron spectroscopy (XPS), extended X-ray absorption fine-structure (EXAFS) analysis, transmission electron microscopy (TEM), and atmospheric gas-phase thiophene HDS.

The issue of the promoter addition effect (high Ni/W ratio required for optimal promotion and very low promotion effect in the case of CoW) was dealt with by

[1] To whom correspondence should be addressed. Fax: **-31-40-2455054. E-mail: Rob.J.A.R.vanVeen@opc.shell.com.

0021-9517/01 $35.00

preparation of Al_2O_3- and TiO_2-supported Ni(Co)W catalysts with different Ni(Co)/W ratios. These catalysts were characterized by atmospheric gas-phase thiophene HDS and Mössbauer emission spectroscopy (MES). For comparison, the activities of Ni(Co)Mo/Al_2O_3 catalysts having different Ni(Co)/Mo ratios were also measured.

EXPERIMENTAL

Catalyst Preparation and Sulfidation

Titania (Degussa P25, extrudates, pore volume 0.32 ml/g, BET surface area 50 m^2/g, anatase : rutile 75 : 25) and alumina (Ketjen CK300, 001-1.5E/3E0.1, extrudates, pore volume 0.66 ml/g, BET surface area 263 m^2/g) were used as supports. Before impregnation, the support materials were calcined for 2 h at 573 K and dried overnight at 383 K. The catalysts were prepared by pore volume coimpregnation with an aqueous solution of $(NH_4)_6W_{12}O_{39} \cdot xH_2O$ and $Ni(Co)(NO_3)_2 \cdot 6H_2O$ followed by drying overnight at 383 K. Subsequently, each catalyst was split into two portions, one of which was calcined at 673 K and the other at 823 K. The calcination was carried out by heating for 1 h to the desired temperature and keeping for 2 h at this temperature.

The Al_2O_3- and TiO_2-supported catalyst contained 15.2 and 7.8 wt% W, respectively. The Ni(Co)/W atomic ratios were 0.1, 0.25, 0.4, and 0.6.

Sulfidation at 1 bar was carried out by heating (6 K/min) the catalysts in 10% H_2S/H_2 (60 ml/min) to the desired temperature (673, 823, or 923 K) and treating them at this temperature for 2 h. The sulfidation at 15 or 30 bar was carried out in 10% H_2S/H_2 (120 ml/min) by heating to 673 K (6 K/min) and treating for 2 h at 673 K. Subsequently, the 15- or 30-bar sulfided samples were flushed 1 h with 1 bar He and transported without exposure to air to a nitrogen recirculation-type glove box (O_2 and $H_2O < 2$ ppm).

For MES measurements, the *in situ* sulfidation at 1 bar was carried out stepwise i.e., 2 h in 10% H_2S/H_2 (60 ml/min) at 298 K, followed by measurement of a Mössbauer emission spectrum, subsequently for 1 h to the next sulfidation temperature, 1 h at this temperature, cooling to room temperature, measurement of a Mössbauer emission spectrum, and so on. The sulfidation temperatures used were 298, 373, 473, 573, 673, and 773 K.

The catalysts are denoted as Co(Ni)W/support(x, y, z), with x, y, and z standing for calcination temperature (T_{cal}), sulfidation pressure (P_{sul}), and sulfidation temperature (T_{sul}), respectively. The Co(Ni)/W atomic ratio is 0.25 unless stated otherwise.

Catalytic Activity

Thiophene HDS measurements were carried out in a microflow reactor under standard conditions (1 bar, 673 K, 4% thiophene/H_2, 50 ml/min). The catalyst was dried at 383 K before use. Subsequently, 200 mg catalyst was mixed with SiC (83 μm) to obtain a bed of 1.5 cm. The samples were *in situ* sulfided in 10% H_2S/H_2 (60 ml/min) by heating (6 K/min) them to the desired temperature (673, 823, or 923 K) and keeping them 2 h at this temperature. The samples sulfided at 823 or 923 K were cooled in 10% H_2S/H_2 (6 K/min) to 673 K. The 15-bar sulfided samples (100 mg) were transferred via a glove box to the microflow HDS equipment without exposure to air and heated (6 K/min) to 673 K (not followed by an isothermal sulfidation step) in 10% H_2S/H_2 (60 ml/min).

After the sulfidation was completed and the reactor temperature reached 673 K the 10% H_2S/H_2 flow was switched to the thiophene/H_2 flow. Reaction products were analyzed in an online gas chromatograph equipped with a CP Sil 5 CB capillary column. The first sample was taken after 2 min reaction time and the following samples at intervals of 35 min. The HDS reaction rate constant per mole of W or Mo was calculated using the total feed (H_2 plus thiophene) flow rate (liters $\cdot$ s^{-1}) at reaction temperature by assuming the reaction to be first order in thiophene (9). The steady-state activities after 10 h run time were compared.

X-Ray Photoelectron Spectroscopy

X-Ray photoelectron spectra were recorded with a VG Escalab 200 spectrometer equipped with an Al$K\alpha$ source and a hemispherical analyzer connected to a five-channel detector. Measurements were carried out at 20-eV pass energy. Charging was corrected for by using the C 1*s* peak at 284.6 eV as a reference. Sulfided samples were ground and pressed in indium foil, which was placed on an iron stub in a glove box. Subsequently, the samples were transferred to a vessel for transport under nitrogen to the spectrometer. The X-ray photoelectron spectra have been fitted with a VGS program fit routine. A Shirley background subtraction was applied and Gauss–Lorentz curves were used.

Transmission Electron Microscopy

Transmission electron microscopy was performed using a Philips CM30 T electron microscope with a LaB_6 filament as source of electrons operated at 300 kV. TEM measurements were carried out on NiW/Al_2O_3(673 K, 1 bar, 923 K) and NiW/Al_2O_3(823 K, 15 bar, 673 K). These samples were taken from the same batches as those used for the EXAFS measurements and were stored in vacuum-sealed ampoules. NiW/TiO_2(673 K, 1 bar, 673 K) and NiW/TiO_2(673 K, 1 bar, 923 K) were sulfided according to the procedure described under Catalyst Preparation and Sulfidation and stored in vacuum-sealed ampoules. The ampoules were opened in a glove box and the samples were mounted on a microgrid carbon polymer supported on a copper grid by placing a few droplets of a suspension of ground sample in *n*-hexane

on the grid. After drying at ambient conditions in the glove box, samples were transferred to the microscope in a special vacuum-transfer sample holder under exclusion of air. An estimation of the distribution in slab length and stacking degree was obtained by examining at least three images of a sample and at least 500 slabs.

Extended X-Ray Absorption Fine Structure

The sulfided catalysts were stored in ampoules under vacuum. These ampoules were opened in a glove box. The samples were mixed with expanded graphite (Lonza HSAG-16) and pressed in self-supporting wafers. The wafers were mounted in vacuumtight sample holders, which were placed in a liquid nitrogen cryostat. Three scans of the W L_{III} edge of each sample were recorded at station 9.2 of the SRS in Daresbury, United Kingdom.

The storage ring was operated at 2.0 GeV; the ring current was in the range 140–250 mA. The Si(220) monochromator was detuned to 50% intensity to remove higher harmonics in the X-ray beam. The absorbance of the Al_2O_3-supported samples was chosen around 2.5. The same data manipulation procedure was used as described in (10, 11). The EXAFS results were produced by fitting in r space until a satisfactory fit was obtained for the k^1- and k^3-weighted FT functions. The various FT ranges used were chosen between 3.3 and 15.7 $Å^{-1}$. The fitting procedures were executed with the XDAP program, Version 2.1.5 (12).

Mössbauer Emission Spectroscopy

MES measurements were performed on CoW/Al_2O_3 (15.2 wt% W, Co/W = 0.6) prepared by incipient wetness impregnation of 299 mg Al_2O_3 with 150 μl of an aqueous solution containing $(NH_4)_6W_{12}O_{39} \cdot xH_2O$ and $Co(NO_3)_2 \cdot 6H_2O$ to which 50 μl of a 26-MBq $^{57}CoCl_2$ (Cynge) solution had been added. The catalyst sample was dried overnight at 383 K and not calcined. Subsequently, it was stepwise sulfided (see Catalyst Preparation and Sulfidation).

All treatments of the MES samples were carried out in an *in situ* reactor which has been described elsewhere (13). However, the heating section as well as the outer container used in this study were made of stainless-steel 316. Furthermore, the reactor was placed horizontally so that a small cup of Vespel (composite material, Du Pont) containing the ground catalyst particles could be mounted easily. After each sulfidation step, Mössbauer emission spectra were recorded at room temperature using a constant acceleration spectrometer in a triangular mode with a single line absorber of $K_4Fe(CN)_6 \cdot 3H_2O$ enriched in ^{57}Fe. The velocity scale was calibrated by using a SNP ($Na_2(Fe(CN)_5NO) \cdot 2H_2O$) absorber and a $^{57}Co:Rh$ source. Positive velocities correspond to the absorber moving away from the source, and the zero of the velocity scale is relative to the single-line position of the $K_4Fe(CN)_6 \cdot 3H_2O$ absorber measured with $^{57}Co:Rh$. The spectra were fitted with calculated subspectra consisting of Lorentzian-shaped lines. The Mössbauer emission spectra of ^{57}Co-doped CoW/Al_2O_3 (not calcined, Co/W = 0.6), were compared with previously measured spectra of ^{57}Co-doped Co/Al_2O_3 (not calcined) (14), and ^{57}Co-doped $CoMo/Al_2O_3$ (T_{cal} = 723 K) (14) and with the Mössbauer absorption spectra of ^{57}Fe-doped NiW/Al_2O_3 (not calcined, Ni/W = 0.25) (6).

RESULTS

Catalytic Activity

The effects of T_{cal} (673 or 823 K) and P_{sul} (1 or 15 bar) on the activity of NiW/Al_2O_3 and NiW/TiO_2 are summarized in Table 1. The following can be deduced:

1. It is clear that all NiW/TiO_2 catalysts (especially those calcined at 673 K) are more active per mole of W than their Al_2O_3-supported counterparts.
2. Irrespective of the support (Al_2O_3 or TiO_2) and P_{sul} (1 or 15 bar) calcination at 823 K instead of at 673 K leads to an activity decrease which is most pronounced for TiO_2-supported catalysts.
3. Increasing P_{sul} from 1 to 15 bar hardly affects the activity of NiW/TiO_2 catalysts (a slight decrease of about 10% was observed), whereas the activity of the 673 K and the 823 K calcined NiW/Al_2O_3 catalysts increases by more than 35%.

Also, T_{sul} had a considerable effect on activity. A peculiar behavior was observed for the TiO_2-supported NiW. Whereas the activity usually decreases with run time, NiW/TiO_2 sulfided at temperatures higher than 673 K showed an activity increase during the first 5 h run time followed by steady-state activity (Fig. 1). For this reason, NiW/Al_2O_3 and NiW/TiO_2 calcined and sulfided at various temperatures were compared based on their steady-state activities measured after 10 h run time (Table 1).

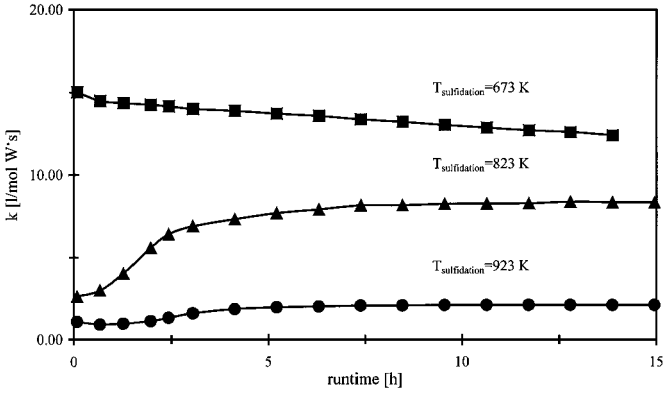

FIG. 1. Thiophene HDS activity as a function of run time for NiW/TiO_2 calcined at 823 K and sulfided (1 bar) at various temperatures.

TABLE 1

Steady-State Thiophene HDS Activity Expressed as k (liters/mol W · s) of Differently Calcined and Sulfided NiW/Al_2O_3 and NiW/TiO_2 Catalysts[a]

	$T^*_{sul} = 673$ K, $P_{sul} = 1$ bar	$T_{sul} = 823$ K, $P_{sul} = 1$ bar	$T_{sul} = 923$ K, $P_{sul} = 1$ bar	$T_{sul} = 673$ K, $P_{sul} = 15$ bar	$T_{sul} = 673$ K, $P_{sul} = 30$ bar
NiW/Al_2O_3 $T_{cal} = 673$ K	7.4 (70% W^{4+})	8.8	8.1 (89% W^{4+})	10.3 (79% W^{4+})	(85% W^{4+})
NiW/Al_2O_3 $T_{cal} = 823$ K	5.9 (49% W^{4+})	9.0	8.3	8.2 (65% W^{4+})	
NiW/TiO_2 $T_{cal} = 673$ K	18.0	8.2	2.3	15.9	
NiW/TiO_2 $T_{cal} = 823$ K	11.0	8.2	2.1	10.1	

[a] For some NiW/Al_2O_3 catalysts the sulfidation degree (% W^{4+}) as determined by XPS is also included.
* T_{cal} = calcination temperature (K). P_{sul} = sulfidation pressure (bar). T_{sul} = sulfidation temperature (K).

The activity of NiW/Al_2O_3 increased on increasing T_{sul} from 673 to 823 K and slightly decreased on a further increase to 923 K. It turned out that the activity is no longer dependent on T_{cal} after sulfidation at 823 or 923 K. The activity of TiO_2-supported NiW strongly decreased with increasing sulfidation temperatures (Table 1, Fig. 1). As for NiW/Al_2O_3, the effect of T_{cal} on activity disappeared after sulfidation at 823 and 923 K.

Activity as a function of promoter/W(Mo) ratio for Al_2O_3-supported CoW, CoMo, NiW, and NiMo, as well as for TiO_2-supported NiW and CoW, is depicted in Figs. 2A and 2B. For maximum activity of $NiMo/Al_2O_3$, NiW/Al_2O_3, NiW/TiO_2 an Ni/Mo or Ni/W ratios of, respectively, 0.3, $\geq$0.6, and 0.4 were required. On the other hand, CoW/TiO_2 and especially CoW/Al_2O_3 showed no clear optimum. In addition, the observed activities of CoW/Al_2O_3 are about equivalent to the lumped activities of W/Al_2O_3 and Co/Al_2O_3.

X-Ray Photoelectron Spectroscopy

The sulfidation degree calculated by dividing the area derived from fitting the 4*f* signal of W^{4+} (the oxidation state of W in WS_2) by that of the total W 4*f* signal (W^{4+} and W^{6+}) is tabulated in Table 1. The sulfidation degree of the various Al_2O_3-supported NiW catalysts clearly depended on T_{cal}, P_{sul}, and T_{sul}. As can be expected, a lower T_{cal} and/or a higher P_{sul} and/or a higher T_{sul} resulted in a higher percentage W present as W^{4+} (thus more W sulfided).

An attempt was also made to determine the sulfidation degree of several NiW/TiO_2 catalysts in this way. However, it was not possible to determine the various X-ray photoelectron spectral areas due to overlap of the Ti 3*p* and W 4*f* signals. In addition, measuring the W 4*d* signal resulted in broad peaks with a low intensity, which caused difficulties with fitting.

Transmission Electron Microscopy

TEM measurements were carried out on NiW/Al_2O_3 (673 K, 1 bar, 923 K) and NiW/Al_2O_3(823 K, 15 bar, 673 K). Representative examples of the images are given in Figs. 3A and 3B. The distributions in stacking degree and slab length of both samples are presented in Fig. 4. NiW/Al_2O_3(673 K, 1 bar, 923 K) had more stacking and longer slabs than NiW/Al_2O_3(823 K, 15 bar, 673 K).

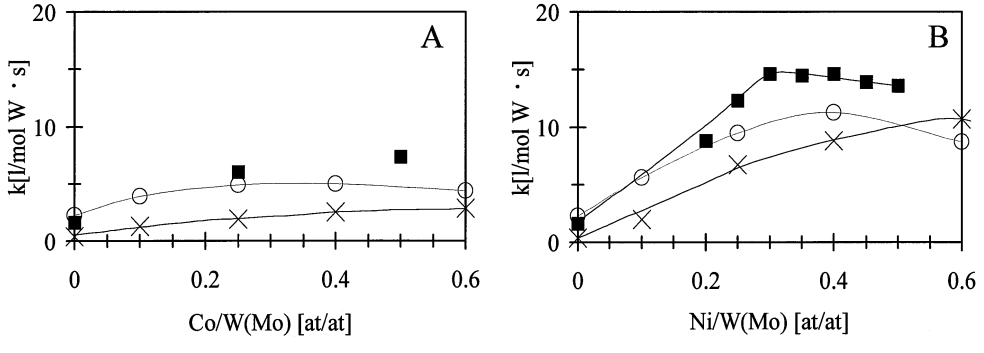

FIG. 2. Activity as a function of promoter/W(Mo) ratio: (A) ■, $CoMo/Al_2O_3$(723 K, 1 bar, 673 K); ○, CoW/TiO_2(823 K, 1 bar, 673 K); ×, CoW/Al_2O_3(823 K, 1 bar, 673 K). (B) ■, $NiMo/Al_2O_3$(723 K, 1 bar, 673 K); ○, NiW/TiO_2(823 K, 1 bar, 673 K); ×, NiW/Al_2O_3(823 K, 1 bar, 673 K).

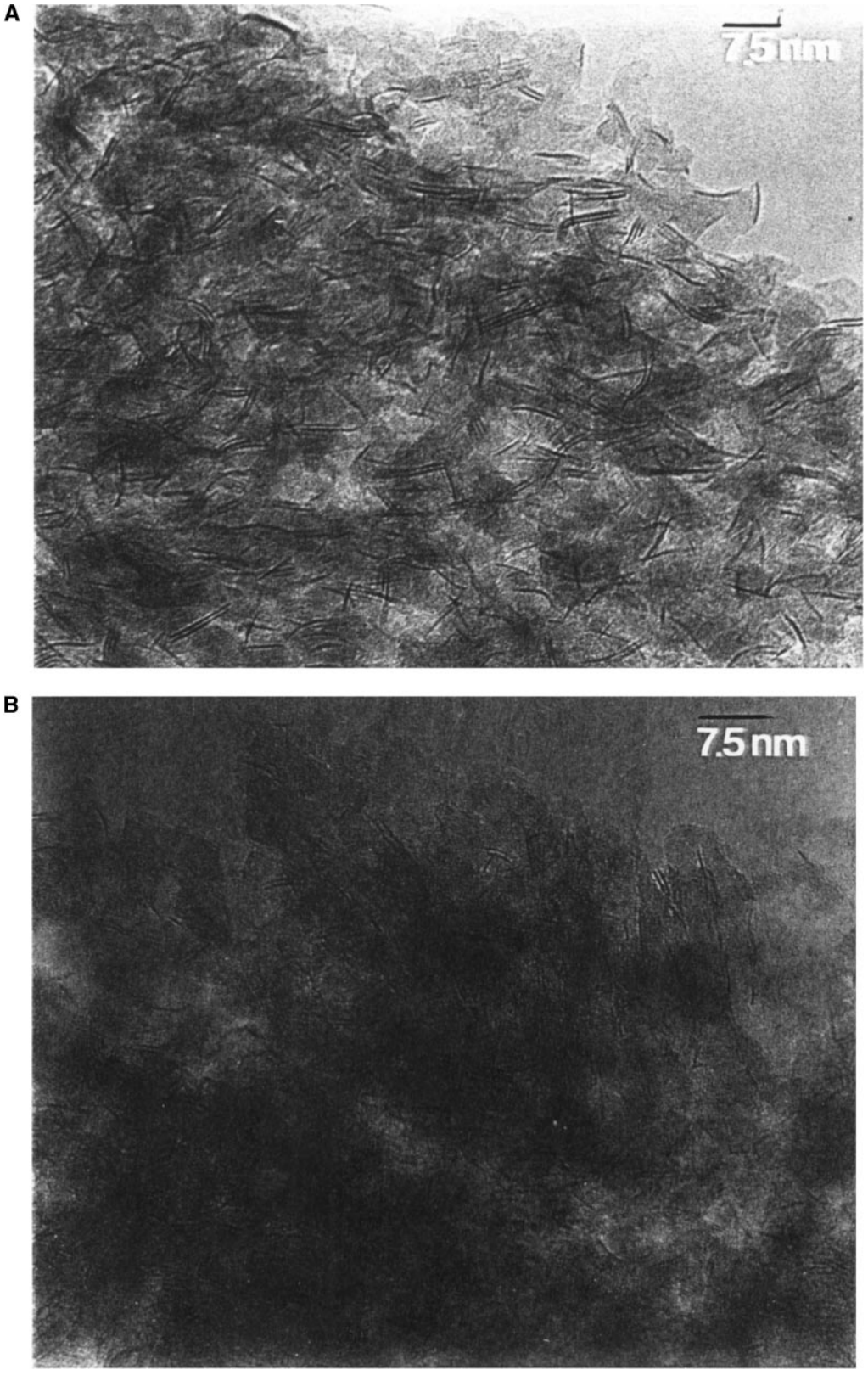

FIG. 3. TEM images of (A) NiW/Al_2O_3(673 K, 1 bar, 923 K) and (B) NiW/Al_2O_3(823 K, 15 bar, 673 K).

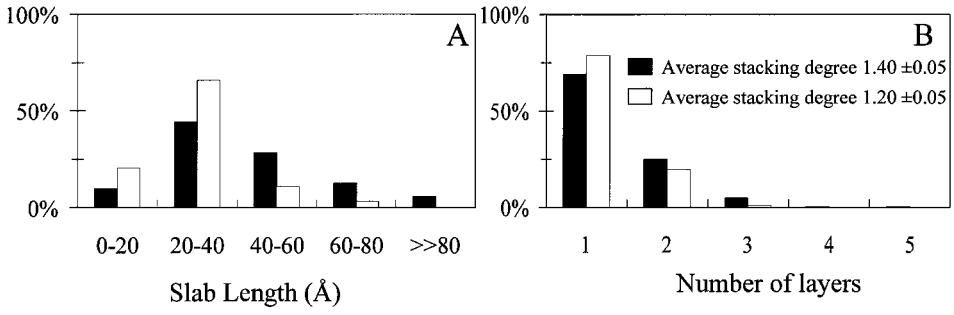

FIG. 4. Distribution in slab length (A) and stacking degree (B) of (■) NiW/Al_2O_3(673 K, 1 bar, 923 K) and (□) NiW/Al_2O_3(823 K, 15 bar, 673 K).

TEM measurements were also carried out on NiW/TiO_2 (673 K, 1 bar, 673 K) and NiW/TiO_2(673 K, 1 bar, 923 K). In both samples single and stacked slabs were observed. The higher T_{sul} (923 K instead of 673 K) did not affect the stacking degree but resulted in an increase in slab length. Careful examination of several photos showed that in contrast to NiW/TiO_2(673 K, 1 bar, 923 K), the WS_2 striae in NiW/TiO_2(673 K, 1 bar, 673 K), which at first site looked like normal-sized slabs, consisted of several smaller ones. This hampered quantitative evaluation of the TiO_2-supported catalysts. After sulfidation at 923 K, the WS_2 slabs on TiO_2 looked larger than on Al_2O_3. Representative transmission electron micrographs of NiW/TiO_2(673 K, 1 bar, 673 K) and NiW/TiO_2(673 K, 1 bar, 923 K) are shown in Figs. 5A and 5B, respectively.

Extended X-Ray Absorption Fine Structure

EXAFS measurements (W L_{III} edge) were carried out on the NiW/Al_2O_3 catalysts presented in Table 2. Their k^3-weighted radial distribution functions together with that of crystalline WS_2 are presented in the Figs. 6 and 7.

From the radial distribution functions of NiW/Al_2O_3(673 K, 1 bar, 923 K), NiW/Al_2O_3(823 K, 15 bar, 673 K), and NiW/Al_2O_3(823 K, 1 bar, 673 K) shown in Fig. 6 it is obvious that the total spectral intensity of the first catalyst is much larger than that of the last two. The two main peaks in the radial distribution function can be ascribed to a "W–S" contribution at 2.41 Å and a "W–W" contribution at 3.16 Å. By analyzing the NiW/Al_2O_3 spectra with these single-backscatterer contributions as obtained from the spectrum of crystalline WS_2, the coordination numbers N_{W-S} and N_{W-W} have been deduced and are listed in Table 2. The coordination numbers of NiW/Al_2O_3(673 K, 1 bar, 923 K) are the same as found for crystalline WS_2 ($N_{W-S} = 6.0$ and $N_{W-W} = 6.0$). This is in line with the TEM images (Fig. 3A) that show the presence of many rather large WS_2 slabs. However, the radial distribution function as presented in Fig. 6 shows that NiW/Al_2O_3(673 K, 1 bar, 923 K) is still less well ordered than the crystalline WS_2 sample. The low coordination numbers for the catalyst calcined at 823 K might indicate that highly dispersed WS_2 was formed. However, the TEM images (Fig. 3B) show that the WS_2 slabs were not that small. It is more likely that these low coordination numbers are due to structural and/or compositional disordering (15). In addition, it should be taken into account that the spectral intensity of the radial distribution function is very weak in the case W has "O" nearest neighbors (as in WO_3) (see, for instance, Fig. 7, $T_{sul} = 573$ K, and (16)). The combination of local/structural disordering and visible WS_2 slabs can be explained by the results of Stockmann *et al.* (17), who showed by image calculations that the WS_2 TEM image was not strongly affected after exchange of one row S by O as long as the structure of the WS_2-like identity was maintained.

To take into account the observed existence of WS_2 slabs in all samples, the EXAFS spectra were fitted in a way different from that normally applied in the literature. Instead of analyzing the spectra with single-backscattering contributions of "S" and "W", the spectra were analyzed by using both the first W–S and the first W–W contribution of the spectrum of crystalline bulk WS_2 as a reference. As a result, it turned out that in addition to a percentage of relatively ordered WS_2, an extra "W–S" contribution had to be included to improve the fitting results. The results obtained in this way are also presented in Table 2

TABLE 2

EXAFS Results of Differently Calcined and Sulfided NiW/Al_2O_3 Catalysts

Catalyst (T_{cal}, P_{sul}, T_{sul})[a]	Routine analysis		Analysis using WS_2 as reference	
	N_{W-S}	N_{W-W}	% WS_2	N_{W-S} in WO_xS_y
NiW/Al_2O_3(673, 1, 923)	6.0	6.0	92	1.7
NiW/Al_2O_3(823, 15, 673)	4.6	3.2	50	3.2
NiW/Al_2O_3(823, 1, 673)	3.4	2.9	49	1.0
NiW/Al_2O_3(823, 1, 573)[b]	—	—	—	—

[a] T_{cal} = calcination temperature (K). P_{sul} = sulfidation pressure (bar). T_{sul} = sulfidation temperature (K).

[b] Intensity of the radial distribution function was to weak to allow analysis. Estimated accuracy N ±20%.

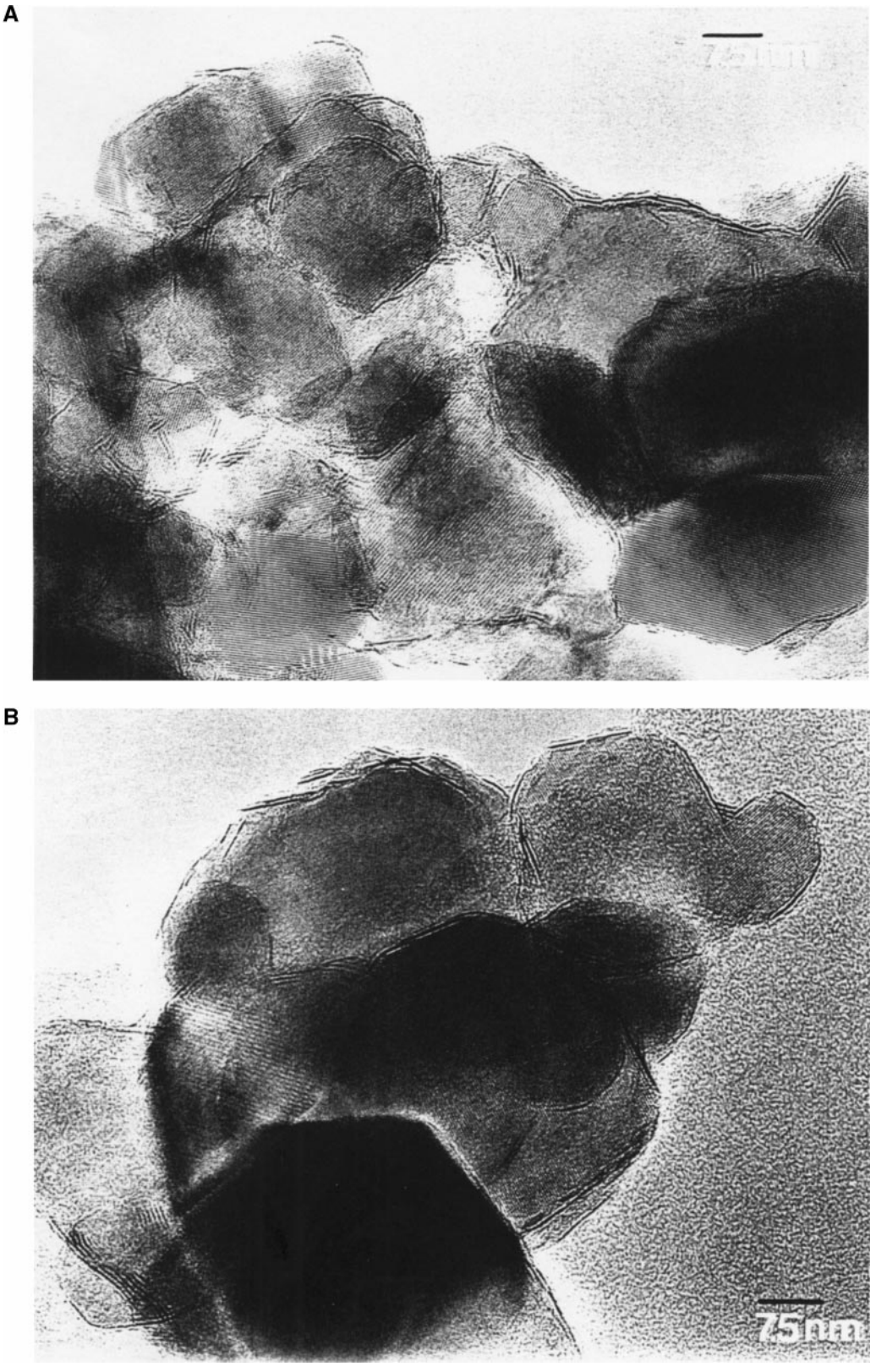

FIG. 5. TEM images of (A) NiW/TiO_2(673 K, 1 bar, 673 K) and (B) NiW/TiO_2(673 K, 1 bar, 923 K).

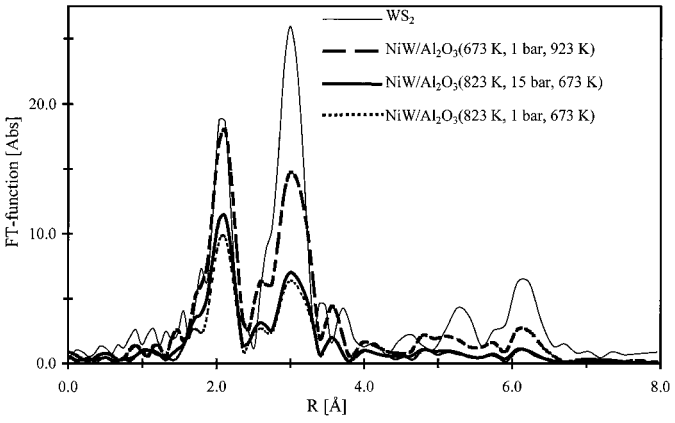

FIG. 6. Uncorrected k^3-weighted-FT functions of crystalline WS_2, NiW/Al_2O_3(673 K, 1 bar, 923 K), NiW/Al_2O_3(823 K, 15 bar, 673 K), and NiW/Al_2O_3(823 K, 1 bar, 673 K).

and have to be interpreted as follows: NiW/Al_2O_3(823 K, 15 bar, 673 K) contained 50% WS_2 and the remaining 50% consists of partially sulfided W particles in which each W atom is surrounded by an average of 3.2 S atoms and no W atoms.

According to this analysis method, NiW/Al_2O_3(673 K, 1 bar, 923 K) was found to contain 92% of "ordered" WS_2 ($N_{W-S} = 6$ and $N_{W-W} = 6$). NiW/Al_2O_3(823 K, 15 bar, 673 K) and NiW/Al_2O_3(823 K, 1 bar, 673 K), which were calcined at a higher temperature ($T_{cal} = 823$ K), seemed to consist of 50% ordered WS_2. Sulfidation at 15 bar instead of 1 bar resulted in an increase in the S surrounding in partially sulfided W phase from 1.0 for $P_{sul} = 1$ bar to 3.2 for $P_{sul} =$ 15 bar.

In fact, the percentages of ordered WS_2 deduced from the k^3-weighted FT functions are determined in this way by scaling the "W–W" contributions to that of the ordered WS_2 reference material ($N_{w-w} = 6$). For simplicity, the distribution of partially sulfided W phases is called WO_xS_y phase.

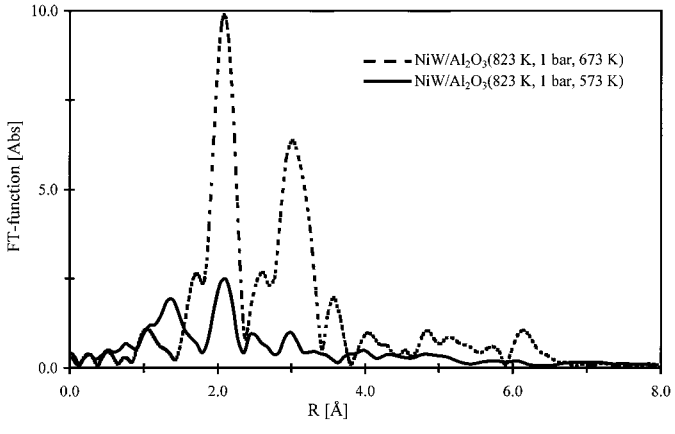

FIG. 7. Uncorrected k^3-weighted-FT functions of NiW/Al_2O_3(823 K, 1 bar, 673 K) and NiW/Al_2O_3(823 K, 1 bar, 573 K).

Although "W–O" contributions could not be deduced from the EXAFS spectra due to the relatively low backscattering contribution of "O", it follows from the XPS results that oxygen is present in the partially sulfided W phases. In addition, the deduced deviations of N_{W-W} and N_{W-S} (see Table 2) and the observation that NiW/Al_2O_3(673 K, 1 bar, 923 K) is still less well ordered than the crystalline WS_2 reference sample are strong indications that we are dealing with a partially sulfided WO_xS_y phase instead of a mixture of WS_2 and W oxide.

Mössbauer Emission Spectroscopy

The Mössbauer emission spectra of CoW/Al_2O_3 sulfided at different temperatures are presented in Fig. 8. Roughly speaking the spectrum of the fresh uncalcined catalyst consisted of two quadrupole doublets, one high-spin 2^+ doublet and one due to either a low-spin 2^+ or a 3^+ phase (18). The spectrum recorded after exposure of the catalyst to the sulfidation gas mixture at 300 K showed that the Co is already completely sulfided, in contrast with uncalcined Co/Al_2O_3 and $CoMo/Al_2O_3$ (14). This spectrum could be analyzed by one quadrupole doublet with a rather large QS value of 0.91 mm/s. After sulfidation at 373 K, the same spectrum was measured. However, at higher T_{sul} the shape of the spectra clearly changed. The overall QS value decreased and the spectrum became asymmetric with increasing T_{sul}. These spectra could be analyzed with three different quadrupole doublets, indicating a distribution in particle size/ordering of the Co-sulfide species formed. One of these doublets resembled the QS value of bulk Co_9S_8, indicating the formation of rather large "Co_9S_8" entities. The amount of Co_9S_8 formed increases from 23% after sulfidation at 473 K to 75% after sulfidation at 773 K.

DISCUSSION

Our XPS and thiophene HDS results (Table 1) are in good agreement with those described by Breysse *et al.* (1, 2), Scheffer *et al.* (3), and Reinhoudt *et al.* (5, 7) in that (i) NiW/Al_2O_3(673 K, 1 bar, 673 K) having the highest W sulfidation degree (70% W^{4+}) was considerably more active than NiW/Al_2O_3(823 K, 1 bar, 673 K) containing only 49% W^{4+}, and (ii) the increase in T_{cal} has a negative effect on activity whereas the effect of an increase in T_{sul} is positive up to a certain T_{sul} level.

As demonstrated in the present paper sulfidation can also be improved by increasing P_{sul}. The advantage of varying P_{sul} is that the effect of T_{sul} changes in W dispersion/sintering can be prevented and the effect of the W sulfidation degree can be more selectively studied. The activity clearly increased after sulfidation at 15 bar (Table 1). NiW/Al_2O_3(673 K, 15 bar, 673 K) and NiW/Al_2O_3(823 K, 15 bar, 673 K) were considerably more active than their 1-bar sulfided counterparts. XPS measurements showed that

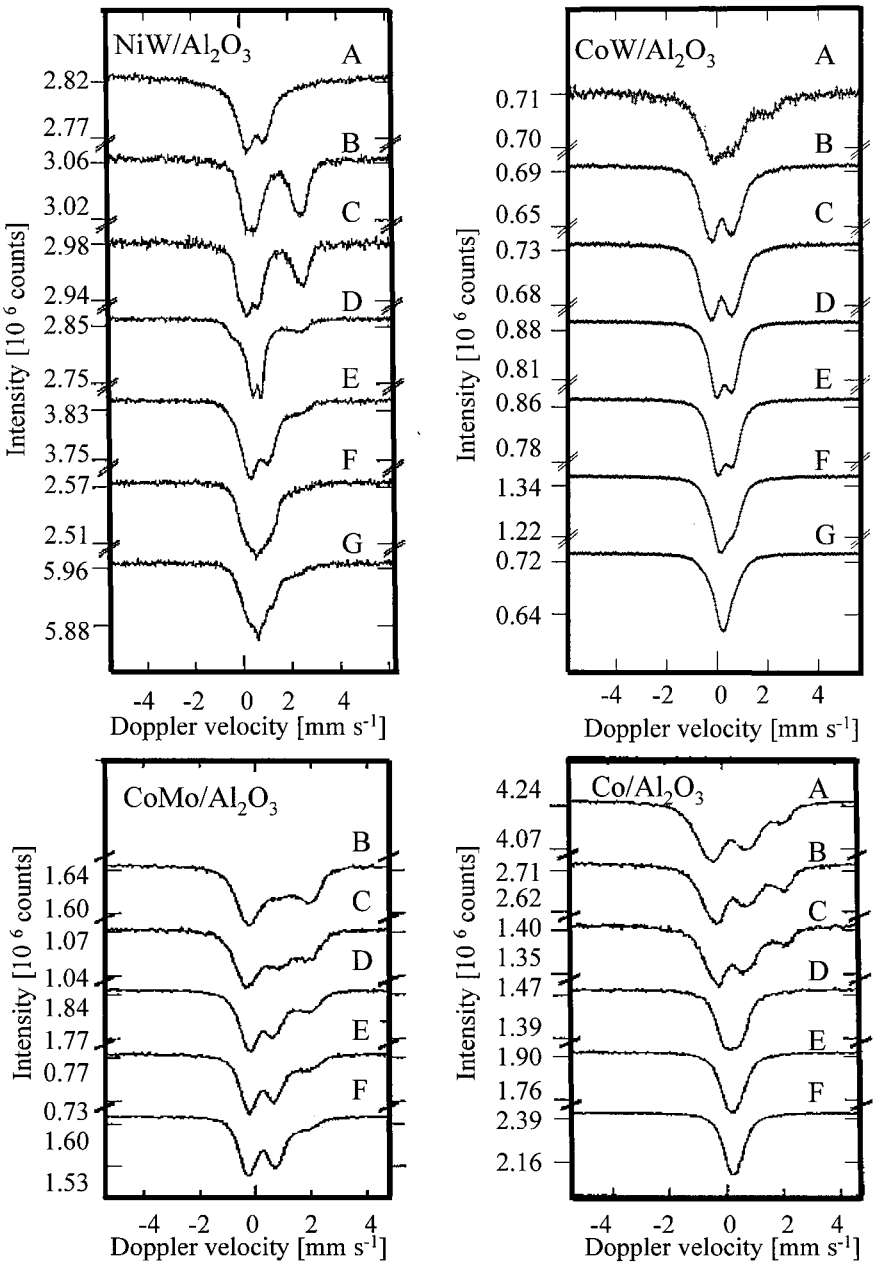

FIG. 8. Mössbauer emission spectra of CoW/Al_2O_3 (not calcined, Co/W = 0.6), Mössbauer absorption spectra of ^{57}Fe-doped NiW/Al_2O_3 (not calcined, Ni/W = 0.25) (6), Mössbauer emission spectra of $CoMo/Al_2O_3$ (T_{cal} = 723 K) (14), and Mössbauer emission spectra of Co/Al_2O_3 (not calcined) (14) recorded after sulfidation at different temperatures. T_{sul}: (A) fresh, not sulfided; (B) 298 K; (C) 373 K; (D) 473 K; (E) 573 K; (F) 673 K; (G) 773 K.

the W sulfidation degree of the 15-bar sulfided samples was higher than that of the 1-bar sulfided samples (Table 1).

These data point to a correlation between activity and W sulfidation degree for catalysts calcined at various temperatures. However, when, in addition to T_{cal}, T_{sul} and/or P_{sul} also were varied, this correlation no longer held. It can therefore be concluded that sulfidation degree is not the only factor determining activity. The most obvious other factor is dispersion differences. Proof of sintering was found by comparing NiW/Al_2O_3(673 K, 1 bar, 923 K) and NiW/Al_2O_3(823 K, 15 bar, 673 K). Although according to XPS, the sulfidation degree of NiW/Al_2O_3(673 K, 1 bar, 923 K) was higher (89%) than the sulfidation degree of NiW/Al_2O_3(823 K, 15 bar, 673 K) (65%), comparable activities (k_{hds} = 8.1–8.2) were found. In addition, the EXAFS data in Table 2 show that NiW/Al_2O_3(673 K, 1 bar, 923 K) contained 92% WS_2 while NiW/Al_2O_3(823 K, 15 bar, 673 K) contained only 50% WS_2. The TEM images clearly show

that WS_2 in NiW/Al_2O_3(673 K, 1 bar, 923 K) was less dispersed than in NiW/Al_2O_3(823 K, 15 bar, 673 K). Longer slabs and a higher stacking degree were found for the former (Figs. 3A, 3B, and 4). Most probably, the much higher T_{sul} induced sintering. By means of electron microscopy Breysse *et al.* (1) compared NiW/Al_2O_3 sulfided at 673 and 773 K and found no important effect of T_{sul} on crystallite size. After sulfidation at 933 K they observed a slight lateral growth (2) but no increase in stacking degree. Reinhoudt *et al.* (5) concluded that up to $T_{sul} = 673$ K mainly subnanometer clusters and nanometer particles are present and that at higher T_{sul} these clusters and particles disappear in favor of WS_2 slab formation. So, most probably, WS_2 sintering starts above 773 K.

With respect to the effect of sulfidation degree on activity, it is interesting to note that the EXAFS results (obtained by using WS_2 as reference) suggested that NiW/Al_2O_3(823 K, 1 bar, 673 K) and NiW/Al_2O_3(823 K, 15 bar, 673 K) both consist of 50% WS_2 (with $N_{W-S} = 6$ and $N_{W-W} = 6$) and that the only difference is the S surrounding of the remaining W. This indicates that the increase in sulfidation degree as determined by XPS from 49% for $P_{sul} = 1$ bar to 65% for $P_{sul} = 15$ bar is caused not by formation of more well-crystallized WS_2 but by formation of a further sulfided WO_xS_y phase which caused the activity increase. In addition, NiW/Al_2O_3(823 K, 15 bar, 673 K), which had a sulfidation degree of 65%, showed higher activity ($k_{hds} = 8.2$) than NiW/Al_2O_3(673 K, 1 bar, 673 K) ($k_{hds} = 7.4$), with a slightly higher sulfidation degree (70%). Possibly, the WS_2/WO_xS_y ratio is different. It can be imagined that a stronger interaction (caused by a higher calcination temperature) delays the sulfidation, resulting in preservation of more WO_xS_y phase.

The WS_2/WO_xS_y ratio can be used to explain the disappearence of the activity difference between NiW/Al_2O_3 samples calcined at 673 or 823 K after being sulfided at 923 K. If T_{sul} becomes higher than T_{cal}, the WS_2/WO_xS_y ratio of the sulfided catalyst is determined primarily by the severity of the sulfidation conditions. In other words, after sulfidation at $T_{sul} \geq 823$ K the same WS_2/WO_xS_y ratios were obtained for $T_{cal} = 673$ K and $T_{cal} = 823$ K.

In conclusion, a higher sulfidation degree of WO_xS_y is favorable for thiophene HDS activity, although complete sulfidation results in WS_2 that is more susceptible to sintering. This sintering effect is strongly induced by high T_{sul}. Prevention of sintering yet achievement of a high sulfidation degree can be obtained by a low T_{cal}, relatively low T_{sul}, and high P_{sul}.

Another way of achieving a high sulfidation degree of W is by preventing formation of strong W–O–support bonds. It was shown by equilibrium adsorption measurements (8) that tungstate hardly adsorbed on TiO_2. This was explained by the presence of mainly coordinatively unsaturated sites (CUSS) at the TiO_2 surface while tungstate prefers electrostatic coordination to acidic OH_2^+ groups. Accordingly, after impregnation and calcination almost no interaction between W and TiO_2 occurs and sulfidation is easier than on Al_2O_3, which shows considerable reactivity toward tungstate. In addition, Ramírez and Gutiérrez-Alejandre reported that TiO_2-supported W could be more easily reduced (19) and sulfided (20) than Al_2O_3-supported W.

Based on the above findings it is to be expected that at 1 bar most of the W in NiW/TiO_2 is sulfidable and that sulfidation at 15 bar does not result in a significantly higher sulfidation degree. Our thiophene HDS results were in agreement herewith. Increasing P_{sul} had only negligible (negative) influence on the activity of NiW/TiO_2 (Table 1). Possibly, higher P_{sul} accelerated the sulfidation as a result of which sintering could occur.

The HDS activity of the TiO_2 catalyst calcined at 673 K ($k_{hds} = 18.0$) was higher than that of the catalyst calcined at 823 K ($k_{hds} = 11.0$) (Table 1). This activity difference is not expected to be caused by a difference in sulfidation degree because of the absence of a P_{sul} effect. Also, it seems unlikely that a transition of anatase to rutile induced by the increase in T_{cal} is the reason for the observed activity difference since the anatase–rutile transition occurs above 923 K (21). In addition, XRD measurements showed that TiO_2 samples (untreated, calcined at 673 K or 823 K, and sulfided at 923 K) all had the same anatase:rutile ratio, namely, 75 : 25. Most likely, the activity difference can be explained by sintering during calcination. Because of the weak bonding between tungstate and TiO_2, tungstate shows some mobility, which increases with higher T_{cal}.

The strong activity decrease on increasing T_{sul} from 673 to 823 or 923 K (Table 1) strengthened the suggestion of sintering with increasing temperature. Due to the weak interaction between tungstate and TiO_2, WS_2 is easily formed and since WS_2 also does not interact with the support, it sinters. This is in agreement with the TEM results (Figs. 5A and 5B) showing that raising T_{sul} from 673 to 923 K results in an increased slab length, while the stacking degree remains unaffected. As in the case of NiW/Al_2O_3, an activity difference between $T_{cal} = 673$ K and $T_{cal} = 823$ K was not observed at $T_{sul} = 823$ K and $T_{sul} = 923$ K. This suggests that after sulfidation at these temperatures the same sulfide phases are formed irrespective of T_{cal}.

Remarkably, the activity of the NiW/TiO_2 catalyst sulfided at 823 or 923 K increased in the first 5 h (Fig. 1). A possible explanation could be that during sulfidation WS_2 sinters due to its weak interaction with the support. Because of this sintering and the high temperature, nickel segregates and forms bulk nickel sulfide. After sulfidation the catalyst was cooled to 673 K (reaction temperature). Possibly, at 673 K a slow redispersion of the NiS to the WS_2 edges occurred, causing an increase in activity. The WS_2 slabs are not expected to fragment at lower temperatures. This suggests that the redispersion of NiS induced by the temperature

is a consequence of the temperature dependency of the strength of interaction between NiS and WS_2.

Summarizing, the NiW/TiO_2 activity results can be explained by a weak interaction between tungstate and TiO_2 resulting in easy sulfidation. A disadvantage of such a weak interaction could be that the WS_2 particles are mobile and susceptible to sintering. To check this and to answer the question why NiW/TiO_2 is more active than NiW/Al_2O_3 detailed structural characterization (e.g., EXAFS) is necessary. These techniques could provide information about the sulfidation degree and morphology. Ramírez and Gutiérrez-Alejandre (19, 20) suggested that the relatively high activity of NiW/TiO_2 is partly caused by differences in dispersion, morphology, and electronic structure induced by the support. Also for Mo-based catalysts it was concluded that the TiO_2 support acts as a promoter (22).

The promotion effect of Co and Ni on W was clearly different from their effect on Mo as can be seen in Figs. 2A and 2B. The following two differences were the most remarkable. First, the optimum Ni/W(Mo) ratio for maximum activity was 0.6 for NiW/Al_2O_3 and 0.3 for $NiMo/Al_2O_3$. Second, the absolute activity increase after addition of increasings amount of Co was much less for W than for Mo. In addition, the lumped activity of Co/Al_2O_3 and W/Al_2O_3 appeared to be similar to the activity of CoW/Al_2O_3. This suggests that (almost) no highly active CoWS phase comparable to the well-known CoMoS phase was formed.

Three possible explanations can be given for the different promotion of W. First, already in the oxidic precursor two separated phases (WO_3 and Co_3O_4 or NiO) might be present. During sulfidation, the corresponding bulk sulfide compounds are formed and no promotion effect is observed. Second, the sulfidation sequence of the W and Co or Ni compounds might not be favorable. The sulfidation of W starts at a much higher temperature than that of Mo. Co and Mo in CoMo are sulfided simultaneously. In several studies (23–25), it was shown that by using a complexing agent the sulfidation of Co was retarded until MoS_2 slabs were formed and that this resulted in a more effective formation of the active CoMoS phase. In CoW catalysts, Co is sulfided before WS_2 slabs are formed and thermodynamically stable Co_9S_8 with a low activity is obtained. Third, the CoWS or NiWS phase is not thermally stable and segregates at high temperatures into WS_2 and Co_9S_8 or Ni_3S_2. Kim *et al.* (26) suggested that the NiWS phase was more thermally fragile than the CoMoS phase. The absence of a promotion effect for $CoWS/Al_2O_3$ suggests then that the CoWS phase is even more thermally fragile than NiWS.

Comparison of the Mössbauer spectra (Fig. 8) of CoW/Al_2O_3, NiW/Al_2O_3 doped with ^{57}Fe (6), $CoMo/Al_2O_3$ (14), and Co/Al_2O_3 (14) allows one to discriminate between the three different possibilities mentioned above. The first explanation based on the presence of two separated phases seems unlikely. In contrast to $CoMo/Al_2O_3$ and Co/Al_2O_3, in the Mössbauer spectra of CoW/Al_2O_3 the high-spin 2^+ contribution indicating a Co–oxygen interaction had already disappeared completely after sulfidation at 298 K. This indicates that W prevented an interaction/reaction between Co and Al_2O_3, for example, by covering the Al_2O_3 surface. This is in line with the suggestion that an interaction between Co and W exists in oxidic CoW/Al_2O_3 (27, 28). Interestingly, also for Ni–W such an interaction was claimed in oxidic NiW/Al_2O_3 (28, 29). Preliminary Raman results showed that the position of the W=O stretching band at around 970 cm^{-1} shifts to a slightly higher wavenumber going from W/Al_2O_3 to CoW/Al_2O_3 or NiW/Al_2O_3. This also points to an interaction between Co(Ni) and W. The observation that the intensity of the W=O signal in CoW/Al_2O_3 was much weaker than that of NiW/Al_2O_3 may indicate that the interaction between Co and W is stronger or that Co is situated on top of the adsorbed WO_x species. According to the MES measurements the sulfidation behavior of CoW/Al_2O_3 is rather similar to that of Co/Al_2O_3 at higher temperatures (14). The Mössbauer emission spectra of Co/Al_2O_3 showed the formation of large and/or well-ordered Co_9S_8 particles (14). However, the spectra of CoW/Al_2O_3 changed more gradually from a doublet with a large QS value (indicating the presence of small/less ordered CoS_x particles) at low T_{sul} to one broad peak (implying that the QS decreased and the particles became larger and/or better ordered) after sulfidation at 773 K.

Comparison of the ^{57}Co-doped CoW/Al_2O_3 Mössbauer emission spectra and the ^{57}Fe-doped NiW/Al_2O_3 Mössbauer absorption spectra (6) shown in Fig. 8 suggests that the presence of W had a different effect on the sulfidation of Co and Ni. The characteristics of the CoW/Al_2O_3 Mössbauer emission spectra recorded at increasing T_{sul} indicated a gradual change from small/less ordered particles to larger/better ordered particles. The absorption spectra of ^{57}Fe-doped NiW/Al_2O_3 indicated a redispersion of the Ni-sulfide particles already formed after sulfidation at 473 K to NiWS as soon as the W started to sulfide at 573 K. Although it will be never possible to prove beyond any doubt that ^{57}Fe behaves similarly to Ni in this catalyst it has been shown before (30) that the ^{57}Fe-doping Mössbauer absorption spectroscopy (MAS) technique could be used to investigate the structure of Ni-containing catalysts like the ^{57}Co doping MES technique applied earlier (31). From the combined MES and MAS results we concluded that the CoS_x particles slowly grew while the NiS_x particles redispersed with increasing T_{sul} and that WS_2 behaves differently toward Co and Ni.

The higher Ni/W than Ni/Mo ratio necessary to obtain a maximum in activity for Al_2O_3-supported catalysts can be explained by the sulfidation sequence of W and Ni. Ni was

sulfided first and bulk Ni sulfide was formed but as soon as WS_2 slabs were formed Ni sulfide redispersed and even migrated to these slabs to form NiWS (6). It can be expected that not all bulk Ni sulfide will participate in this redispersion and will migrate to the WS_2 edges. Consequently, a higher Ni loading was required to realize optimal NiWS formation. Interestingly, the optimum Ni/W ratio for NiW/TiO_2 (the sulfidability of W is easier due to less interaction with the support (8)) was lower than that of NiW/Al_2O_3. Most probably, on TiO_2 the WS_2 slabs were formed at lower temperatures and more NiWS phase was formed without bulk Ni sulfide formation preceding, and as a result the optimal Ni/W ratio was closer to the optimal Ni/Mo ratio.

For CoW/Al_2O_3, no redispersion was observed in the MES measurements. This indicates that already at relatively low T_{sul} (below 573 K at which W started to sulfide) Co_9S_8 was formed that was too stable to redisperse to smaller particles. Indeed, the Mössbauer emission spectra point to the formation of Co_9S_8 at low temperatures. After sulfidation at 473 K a spectral contribution of 23% Co_9S_8 was required for a satisfactory fit. This amount increased with increasing T_{sul} (573 K 29% Co_9S_8, 673 K 45% Co_9S_8, 773 K 75% Co_9S_8). The Mössbauer emission spectra of $CoMo/Al_2O_3$ showed at all T_{sul} a doublet. After fitting a large QS value was found, indicating the formation of small and/or less ordered CoS particles (14).

To check the explanation for the optimal promoter/Mo(W) ratio by the ease of formation of WS_2 slabs it is useful to study the optimal ratio for other supports differing in interaction with W.

CONCLUSION

The sulfidation degree of W is clearly an important parameter for the preparation of supported W-based catalysts. This sulfidation degree can be controlled by support, calcination temperature (T_{cal}), sulfidation pressure (P_{sul}), and sulfidation temperature (T_{sul}). However, it is important to realize that the formation of WS_2 proceeds via partially sulfided WO_xS_y. A higher sulfidation degree of the WO_xS_y phase results in a higher thiophene HDS activity. Nevertheless, complete sulfidation of the WO_xS_y phase ends in the formation of WS_2, which is more susceptible to sintering. The amount of sintering is determined by T_{sul} and support interaction. Highest activity in thiophene HDS is obtained for Al_2O_3-supported NiW catalysts by sulfidation at low T_{sul} plus at high P_{sul}. For NiW supported on TiO_2 T_{cal} and T_{sul} have to be low and sulfidation at atmospheric pressure is already sufficient because W is more easily sulfided due to the weak support interaction.

The difficult sulfidation also affects the promotional behavior. The optimal Ni/W ratio is higher than the optimal Ni/Mo ratio, while in contrast to CoMo catalysts, for CoW no optimal Co/W ratio is found. It appeared that during sulfidation of NiW and CoW, Ni and Co were sulfided first. As soon as WS_2 is formed the NiS particles formed partially redisperse to form NiWS, while the CoS_x particles formed tend to form Co_9S_8 instead of CoWS.

We surmise that the weak coordination of W to TiO_2 results in an easy sulfidation causing a more completely sulfided catalyst compared with W/AlO_3. As a result TiO_2-supported catalysts show a higher activity and a lower optimal Ni/W ratio than their Al_2O_3-supported counterparts.

ACKNOWLEDGMENTS

These investigations have been supported by The Netherlands Foundation for Chemical Research (SON) with financial aid from The Netherlands Technology Foundation (STW). The research has been performed under the auspices of NIOK, The Netherlands Institute for Catalysis Research, Lab Report TUE-00-6-02. The authors thank Dr. P. J. Kooyman (National Centre of High Resolution Electron Microscopy, Delft University of Technology) and Mr. M. W. G. M. T. Verhoeven (Eindhoven University of Technology) for conducting TEM and XPS measurements, respectively.

REFERENCES

1. Breysse, M., Bachelier, J., Bonnelle, J. P., Cattenot, M., Cornet, D., Décamp, T., Duchet, J. C., Durand, R., Engelhard, P., Frety, R., Gachet, C., Geneste, P., Grimblot, J., Gueguen, C., Kasztelan, S., Lacroix, M., Lavalley, J. C., Leclercq, C., Moreau, C., de Mourgues, L., Olivé, J. L., Payen, E., Portefaix, J. L., Toulhoat, H., and Vrinat, M., *Bull. Soc. Chim. Bel.* **96**, 829 (1987).
2. Breysse, M., Cattenot, M., Décamp, T., Frety, R., Gachet, C., Lacroix, M., Leclerq, C., de Mourques, L., Portefaix, J. L., Vrinat, M., Houari, M., Grimblot, J., Kasztelan, S., Bonnelle, J. P., Housni, S., Bachelier, J., and Duchet, J. C., *Catal. Today* **4**, 39 (1988).
3. Scheffer, B., Mangnus, P. J., and Moulijn, J. A., *J. Catal.* **121**, 18 (1990).
4. Reinhoudt, H. R., van Langeveld, A. D., Mariscal, R., de Beer, V. H. J., van Veen, J. A. R., Sie, S. T., and Moulijn, J. A., *Stud. Surf. Sci. Catal.* **106**, 263 (1997).
5. Reinhoudt, H. R., van Langeveld, A. D., Kooyman, P. J., Stockman, R. M., Prins, R., Zandbergen, H. W., and Moulijn, J. A., *J. Catal.* **179**, 443 (1998).
6. Reinhoudt, H. R., van der Meer, Y., van der Kraan, A. M., van Langeveld, A. D., and Moulijn, J. A., *Fuel. Proc. Tecnol.* **61**, 43 (1999).
7. Reinhoudt, H. R., van Langeveld, A. D., Moulijn, J. A., and van Veen, J. A. R., *Proc. Symp. 215th ACS Natl. Meet. Div. Petrol. Chem.*, 46 (1998).
8. Vissenberg, M. J., Joosten, L. J. M., Heffels, M. M. E. H., de Beer, V. H. J., van Santen, R. A., and van Veen, J. A. R., *J. Phys. Chem. B.* **104**, 8456 (2000).
9. Duchet, J. C., van Oers, E. M., de Beer, V. H. J., and Prins, R., *J. Catal.* **80**, 386 (1983).
10. de Bont, P. W., Vissenberg, M. J., Boellaard, E., de Beer, V. H. J., van Veen, J. A. R., van Santen, R. A., and van der Kraan, A. M., *J. Phys. Chem. B* **101**, 3072 (1997).
11. de Bont, P. W., Vissenberg, M. J., de Beer, V. H. J., van Veen, J. A. R., van Santen, R. A., and van der Kraan, A. M., *J. Phys. Chem. B* **102**, 5876 (1998).
12. Vaarkamp, M., Linders, J. C., Koningsberger, D. C., to be published.
13. van der Kraan, A. M., and Niemantsverdriet, J. W., *in* "Industrial Applications of the Mössbauer Effect" (G. J. Long and J. G. Stevens, Eds.), p. 609. Plenum, New York, 1986.

14. Crajé, M. W. J., de Beer, V. H. J., van Veen, J. A. R., and van der Kraan, A. M., *J. Catal.* **143**, 601 (1993).
15. Shido, T., and Prins, R., *J. Phys. Chem. B* **102**, 8426 (1998).
16. Kuzmin, A., and Purans, J., *J. Phys. Condens. Matter* **5**, 2333 (1993).
17. Stockmann, R. M., Zandbergen, H. W., van Langeveld, A. D., and Moulijn, J. A., *J. Mol. Catal.* **102**, 147 (1995).
18. Steven, J. G., Zhe, L., Pollak, H., Stevens, V. E., White, R. H., and Gibson, J. L. (Eds.), "Mössbauer Handbook on Minerals," 1983.
19. Ramírez, J., and Gutiérrez-Alejandre, A., *J. Catal.* **170**, 108 (1997).
20. Ramírez, J., and Gutiérrez-Alejandre, A., *Catal. Today* **43**, 123 (1998).
21. JCPDS-ICDD index, International Center for Diffraction Data (1996), PDF-2 Sets 1-46 databases, 21-1272 and 21-1276.
22. Ramirez, J., Cedeño, L., and Busca, G., *J. Catal.* **184**, 59 (1999).
23. Medici, L. A., and Prins, R., *J. Catal.* **163**, 28 (1996).
24. Medici, L. A., and Prins, R., *J. Catal.* **163**, 38 (1996).
25. de Jong, A. M., de Beer, V. H. J., van Veen, J. A. R., and Niemantsverdriet, J. W., *J. Phys. Chem.* **100**, 17722 (1996).
26. Kim, C. H., Yoon, W. L., Lee, I. C., and Woo, S. I., *Appl. Catal. A* **144**, 159 (1996).
27. Zhang, R., Schwarz, J. A., Datye, A., and Baltrus, J. P., *J. Catal.* **135**, 200 (1992).
28. Contescu, Cr., Jagiello, J., and Schwarz, J. A., *J. Phys. Chem.* **97**, 10152 (1993).
29. Southmayd, D. W., Contescu, Cr., and Schwarz, J. A., *J. Chem. Soc. Faraday. Trans.* **89**, 2075 (1993).
30. van der Kraan, A. M., de Jong, M., Crajé, M. W. J., and de Beer, V. H. J., *Hyperfine Interact. C* **3**, 100 (1998).
31. Crajé, M. W. J., de Beer, V. H. J., and van der Kraan, A. M., *Catal. Today* **10**, 339 (1991).